



Green synthesis of nickel oxide nanoparticles and its adsorption isotherm and kinetics studies for heavy metal ions removal

Pratima Rani sardar

Department of Botany, Shivaji College, University of Delhi

New Delhi, India -110027

Email: pratimasardar07@gmail.com

ABSTRACT

A facile synthesis of NiO nanoparticles using a hydrothermal method and evaluate their potential towards the adsorptive removal of Cd (II). Azadirachta indica leave extract was used in this study as a reducing agent. The process is green, generates less amount of toxic by-products, and also require less quantity of chemical as compared to other available methods. The NiO nanostructures were characterized by X-ray diffraction, energy-dispersive X-ray spectroscopy, and scanning electron microscopy. The nitrogen adsorption-desorption BET analysis indicated that the hybrid is mesoporous, having a surface area of 32.60 m².g⁻¹ and a pore diameter of 1.914 nm. The experimental results suggest that the adsorption process is physical and follows the Langmuir isotherm and pseudo-second-order model for metal ion adsorption in single and mixed solutions. Also, the adsorption process is spontaneous and primarily dominated by film diffusion. The NiO showed excellent adsorption of metal ions with a maximum adsorption capacity of ~165 mg.g⁻¹ for cadmium.

Keywords- Green synthesis; NiO nanoparticle; adsorption; heavy metal ions

Received 28.07.2021

Revised 06.08.2021

Accepted 08.08.2021

INTRODUCTION

Uncontrolled discharge of industrial effluents from various industries like battery manufacturing, paints industries, fertilizers [1] causes heavy metal pollution. Long-term exposure to metal ions in the human body causes serious problems like skin disease, nausea, irritations, and damage to the nervous system, liver, kidney [2]. Cadmium (Cd) is considered to be one of the most toxic metal ions that affect the environment and human health severely [3, 4]. Considering the adverse health effect of cadmium ions, Occupational Safety and Health Administration (OSHA) has fixed the permissible exposure limit (PEL) for Cd (II) to 5 µg.m⁻³. Hence, the development of an efficient and cheap treatment method is important to safeguard human health from possible heavy metal poisoning.

There are various techniques available for removing metal ions from the water like membrane separation [5], ion exchange [6], precipitation [7], and electrolysis [8]. However, high cost and maintenance, more energy required are the limitations of these techniques. Compared to these techniques, adsorption is the simplest and most economical process for removing metal ions from water [9, 10]. The efficiency of an adsorption process depends on the adsorption capacity of the adsorbents. Higher specific surface area and the large pore volume of an adsorbent can provide a better adsorption capacity. These properties of the materials also facilitate the mass diffusion and transport of metal ions in the adsorbent, thus enabling the improvement in the performance of metal ion removal from wastewater. Activated carbon [11, 12], zeolites [13], kaolinite [14], alumina [15], and red mud are examples of efficient adsorbents. In recent times, due to the advancement of nanotechnology, the synthesis of high-surface nanoparticles becomes easy, and various nanomaterials have been proposed for heavy metal removal from wastewater [16].

Among the nanoparticle, metal-oxide-based nanoparticles proved to be an excellent material for the removal of metal ions from water because of their high surface area, higher porosity, and small size [16]. Previously, the use of superparamagnetic Fe₃O₄ microspheres for the efficient removal of metal ions was reported by exploiting their magnetic, water-dispersible, and pore-size tuneable properties [17]. MnO₂-coated magnetic nanocomposites (Fe₃O₄/MnO₂) prepared through hydrothermal technique also exhibit good removal properties and can be used as recyclable adsorbent [18]. TiO₂ nanostructures synthesized by hydrolysis of titanium tetrachloride in HCl were used as an adsorbent for the removal of heavy metal ions removal. Adsorption studies show that the maximum adsorption capacity of TiO₂ for the lead was

132.458 mg.g⁻¹[19]. NiO nanoparticles also showed great adsorption behaviour for heavy metal removal[20-22].

The NiO nanoparticle can be synthesized through many routes. Co-precipitation, hydrothermal and solvothermal, sol-gel, and microwave-assisted synthesis methods are a few of them. For example, Zhao et al used the co-precipitation method in presence of ethanolamine [22], Khoshhesab *et. al.* used the co-precipitation method [23], and Qamar et. al. used the sol-gel method[21] to synthesized the high-surface NiO nanoparticles and proved the effectiveness of the nanoparticle for various heavy metal removal. Although, this nanoparticle removes the pollutants from wastewater, their synthesis method involved lot many harsh chemicals which are not environmentally friendly. In some cases, toxic by-products are also generated during the synthesis process. Hence, a green-synthesis process could be an alternative method that can not only reduces the chemical load in the synthesis process but also reduces the by-products generations.

Here, we report a facile synthesis of NiO nanoparticles using a hydrothermal method and evaluate their potential towards the adsorptive removal of Cd (II). The process is green, generates less amount of toxic by-products, and also require less quantity of chemical as compared to other available methods. The NiO nanostructures were characterized by X-ray Diffraction, scanning electron microscopy, and BET surface area analysis. Cd (II) was used as a model heavy metal ion to evaluate the adsorbent's potential. The adsorption data were fitted using Langmuir and Freundlich isotherms model equation, and the time-dependent adsorption data were fitted using pseudo-first-order and pseudo-second-order kinetic equations. Results indicate an excellent removal of cadmium ions from water and provided comparable adsorption capacity with the other published materials.

MATERIAL AND METHOFDS

Experimental

Analytical grade chemicals were used to prepare the sample and to perform the adsorption studies. Nickel nitrate (NiCl₂·6H₂O), cadmium nitrate Cd(NO₃)₂, and absolute ethanol were purchased from Sigma Chemicals.

NiO nanostructure synthesis

Azadirachta indica, commonly known as neem extract was used in this study. The leaves were collected from local surroundings and rinsed with distilled water to remove any associated debris. These clean leaves were then dried, and grinded in a pestle and mortar. 50 g of leaves was refluxed in 1000 mL of ethanol for 24 h and the resulted infusion was filtered using Whatmann filter paper. The filtered extract free from solid particles was then used for the nanoparticle synthesis as reducing agents.

To get the NiO nanoparticle, NiCl₂·6H₂O was added into a solution of ethanol and water (4:1) followed by adjustment of solution pH to 12 by adding NaOH. Then the neem extract was added into the solution and transferred to an autoclave for hydrothermal treatment for 12 hours at 150 °C. The product from the autoclave was then washed and calcined at 300 °C for 1 hr in an inert atmosphere to complete the NiO synthesis.

Characterizations

The X-ray diffraction of the NiO nanoparticles was done for phase identification of crystalline material using CuK_α radiation (λ= 0.15418 nm) (Netherland PANalytical X'Pert PRO diffractometer). The morphology of the nanostructure was captured using field emission scanning electron microscopy (FEI Quanta 200 FE-SEM with a beam energy of 10kV). The elemental composition of the nanomaterial was determined through energy dispersive X-ray stereoscopy (EDS) mapping using the Oxford-EDX system (IE 250 X Max 80). The specific surface area and pore size of the nanomaterial were determined through nitrogen adsorption/desorption isotherms using Nova touch LX² equipment.

Adsorption Study

All the adsorption experiments were conducted in batch mode. All the adsorption experiments were done by adding 2.5 mg of NiO adsorbent into 25 mL of the test solution with varied initial concentrations. For equilibrium studies, the initial concentration of the metal ions was varied from 5 to 400 mg/L. The adsorbent was added to the different metal ions concentrations and left in a shaker for 24 hrs to achieve equilibrium. The samples were then centrifuged and the residue amount of metal ions in the sample was analyzed by the AAS technique. For kinetic experiments, the metal concentration was kept fixed at 100 mg.L⁻¹, and contact time was varied from 5 min to 120 min.

A stock solution (1000 mg.L⁻¹) was used to get the various concentrations of Cd (II) solution using the serial-dilution technique. The residual metal ion concentration in the water was determined by atomic absorption spectroscopy. A calibration curve was plotted to determine the concentration of unknown samples by comparing them to the set of standards of the known concentration samples. A series of standard solutions of various concentration were prepared within the concentration range of the AAS

instrument i.e. 0.5 to 5 mg.L⁻¹. The concentration lies above the range were diluted and then analyzed. A dilution factor was used to calculate the final concentration of the sample. The adsorption yield and adsorption capacity were obtained from the following equations respectively.

$$\text{Removal efficiency (\%)} = \frac{C_0 - C_e}{C_0} \times 100$$

$$q_e = \frac{(C_0 - C_e)}{m}$$

RESULTS AND DISCUSSIONS

Verification of NiO formation

The shape and morphology of the NiO nanostructure were investigated by field-effect scanning electron microscopy. **Figure 1a** illustrates the SEM images of NiO nanostructure. A highly porous structure that forms due to the aggregation of smaller particles together is evident in the SEM image. The EDS spectrum of the NiO was captured to identify the elements present in the nanoparticle. **Figure 1b** illustrates the EDS spectrum of the synthesized nanomaterial. EDS spectra' elemental analysis confirmed the presence of nickel, and oxygen in the hybrid.

The NiO nanostructures were characterized through X-ray diffraction to investigate the phase and crystallinity of the sample. The peaks were observed at a diffraction angle (2θ) of 37.26, 43.29, 62.89, 75.43 and 79.43 corresponds to (111), (200), (220), (311) and (222) for NiO (JCPDS no 78-0643) which confirms the formation of NiO (**Figure 1c**) [24].

The surface area of the NiO nanostructure was determined by the BET surface area analyzer. N₂ adsorption-desorption isotherms were used to calculate the surface area of the sample. **Figure 1d** represents the nitrogen adsorption-desorption isotherms of NiO nanostructure. A significant hysteresis was observed in the BET isotherm. The nature of hysteresis loop similar to a type-IV adsorption isotherm [25], which is generally obtained in case of a mesoporous material. The surface area and pore diameter of the NiO nanostructure was found to be ~32.60 m².g⁻¹ and ~1.9 nm, respectively.

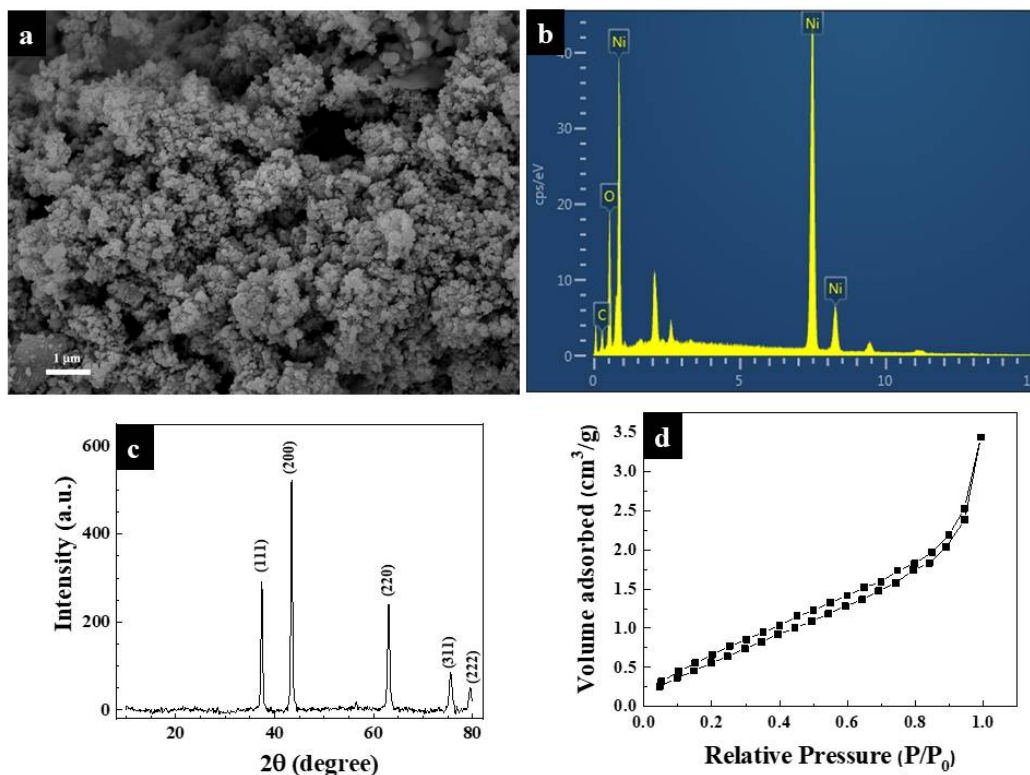


Figure 1:(a) SEM image, (b) EDS spectrum, and (c) XRD pattern, (d) N₂ adsorption-desorption BET (Brunauer-Emmett-Teller) isotherms, of NiO nanoparticle.

Adsorption Kinetics

The kinetic experiment results are presented in **Figure 2a**. An unchanged adsorption capacity was observed after 60 min indicating a 60 min required to attain the equilibrium. Two commonly used kinetics model equations: (i) pseudo-first-order (**Equation1**) and (ii) pseudo-second-order (**Equation2**) models were used to compute the rate constants and other kinetics parameters of the adsorption process[26].

$$\log(q_e - q_t) = \log q_e - \frac{k_1 t}{2.303} \dots \dots \dots (1)$$

$$\frac{t}{q_t} = \frac{1}{k_2 q_e^2} + \frac{t}{q_e} \dots \dots \dots (2)$$

Where q_t (mg.g⁻¹) and q_e (mg.g⁻¹) are the amounts of metal ion adsorbed per unit weight of adsorbent at time t (min) and equilibrium, respectively; k_1 (min⁻¹) and k_2 (g.mg⁻¹.min⁻¹) are the rate constant of pseudo-first-order and pseudo-second-order reaction respectively.

These kinetic experiment data were further fitted using pseudo-first-order and pseudo-second-order model equations and presented in **Figure 2b** and **2c**, respectively. Corresponding parameters of the model equations were also presented in **Table 1**. The higher correlation coefficient(R²) of the pseudo-second-order model compared to the pseudo-first-order model equation suggested that the pseudo-second-order kinetic model could better explain the metal ion adsorption.

Table 1:The kinetic parameters of pseudo-first-order and pseudo-second-order model for Cd (II) adsorption onto NiO

	Pseudo-first-order model		Pseudo- second-order model	
	k ₁ (min)	R ²	k ₂ (× 10 ³ .g.mg ⁻¹ .min ⁻¹)	R ²
Cd(II)	0.036	0.96	1.83	0.99

The kinetic model provides information related to adsorption rate kinetics. However, it failed to provide any information related to the adsorption mechanism. Hence, the kinetic experimental data was further fitted with intraparticle diffusion and Boyd models to have an idea about the rate-controlling step of the process. Intraparticle diffusion model [27, 28], and Boyd model [28] are given by **Equation3**, and **Equation4**.

$$q_t = k_p t^{1/2} + C \dots \dots \dots (3)$$

$$B_t = -0.4944 - \ln(1 - F) \dots \dots \dots (4)$$

Where k_p (mg.g⁻¹.min^{-1/2}) is the intraparticle diffusion rate constant, C is the measure of boundary layer diffusion effect and $F = \frac{q_t}{q_e} = 1 - \frac{6}{\pi^2} \exp(-B_t)$.

The experimental results were fitted with the intra-particle diffusion model and Boyd and presented in **Figure 2d**, and **2e**. The linear fit line intra-particle diffusion model equation provides a low R² value (**Figure 2d**) compared to the Boyd model equation (**Figure 2e**). It is also observed that the Boyd model-fitted lines pass through the origin. These phenomena indicated that the adsorption process is not primarily dominated by intra-particle diffusion, but primarily dominated by film-diffusion resistance[29].

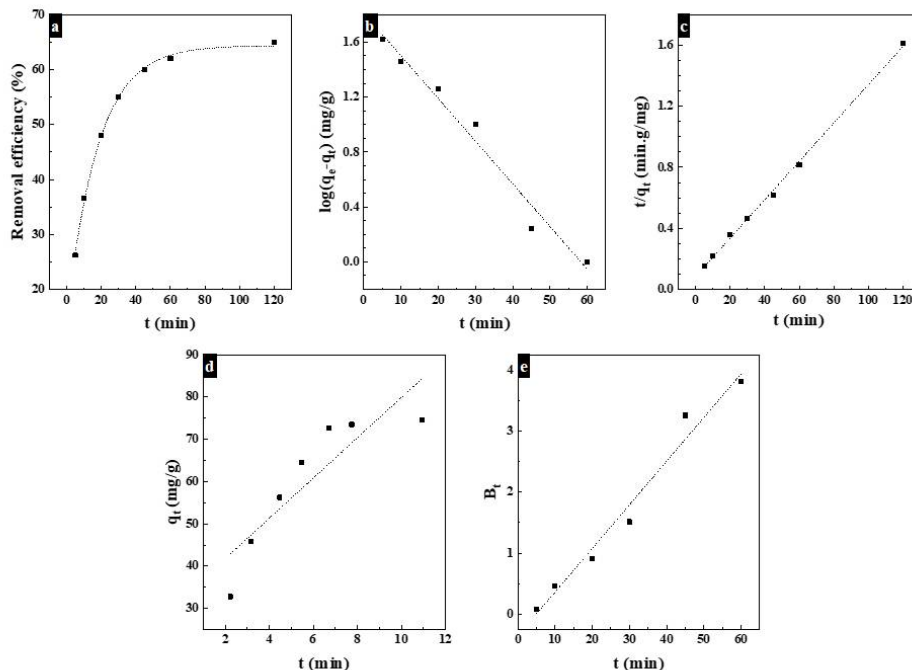


Figure 2:(a) Adsorption capacity of NiO adsorbent for the adsorption of Cd (II) versus time plot. (b) Pseudo-first-order, (c) pseudo-second-order, (d) intra-particle diffusion model ($R^2 = 0.64$), and (e) B_t versus time plot ($R^2 = 0.99$) for initial concentration of 100 mg.L^{-1} of Cd (II).

Adsorption Isotherms

The interaction between the adsorbate and adsorbent is determined by adsorption isotherms. The adsorption data for Cd (II) metal ions were fitted by different adsorption isotherms for metal ion concentrations varying from 5 to 400 mg.L^{-1} . The assumption for Langmuir isotherm is monolayer adsorption i.e. the layer adsorbed on the surface of adsorbate is one molecule in thickness. The adsorption process occurs at a definite number of localized sites and no hindrance between adsorbed molecules takes place. Langmuir isotherm is given as **Equation 5** [30].

$$\frac{C_e}{q_e} = \frac{1}{bq_{max}} + \frac{C_e}{q_{max}} \dots \dots \dots (5)$$

Where q_{max} (mg.g^{-1}) and q_e (mg.g^{-1}) are the maximum metal ions adsorption capacity and adsorbed amount of metal ions at equilibrium condition by the nanomaterials, respectively. b (L.g^{-1}) is the Langmuir adsorption constant. The linear form of Freundlich isotherm is given in **Equation 6**[30].

$$\log q_e = \log k_f + \left(\frac{1}{n}\right) \log C_e \dots \dots \dots (6)$$

Where k_f ($\text{mg.g}^{-1}.\text{L}^{1/n}.\text{mg}^{-1/n}$) and n (dimensionless) are the Freundlich adsorption constants and adsorption coefficient of the system, respectively. The separation factor, $R_L (=1/(1+bC_0))$ is a dimensionless parameter and an indicator of process feasibility. The process is considered to be favorable if the R_L is less than 1 [31].

Figure 3a represents the initial-concentration-dependent Cd (II) adsorption capacities of the nanomaterial. A sharp increase in adsorption capacity with increasing concentration is visible. However, the adsorption capacity was plateaued at a higher metal ion concentration. The maximum adsorption capacity of NiO was found to be $\sim 165 \text{ mg.g}^{-1}$ for Cd (II), which is better than the recently published results (**Table 2**).

Table 2. Comparison of adsorption capacity of NiO with other adsorbents

Adsorbents	Adsorption capacity of Cd (II) (mg.g^{-1})	Ref.
$\text{Fe}_3\text{O}_4\text{-SO}_3\text{H NPs}$	80.9	[9]
Nanorods NiO	95	[6]
Fe_3O_4 NPs	32.0	[30]
$\text{NH}_2\text{-MCM 41}$	18.25	[31]
NiO nanostructure	165	This work

The equilibrium experimental data were fitted with the Langmuir and Freundlich isotherm and shown in **Figure 3b** and **Figure 3c**, respectively. The constants of the respective isotherms were calculated from the C_e/q_e versus C_e plot and $\log q_e$ versus $\log C_e$ plot, respectively, and presented in **Table 3**. A higher value of R^2 and lower values for the Langmuir model fitting than the Freundlich model indicates that the metal ion adsorption can better explain by the Langmuir isotherm model. Further, R_L 's positive values having less than 1 suggested the adsorption of metal ions would be a favourable process [31].

Table 3: The parameter of Langmuir, Freundlich, and DKR isotherm model for Cd (II) adsorption.

Langmuir		Freundlich			DKR		
b (L.mg ⁻¹)	R ²	n	k _f (mg.g ⁻¹)(L ^{1/n} .mg ^{-1/n})	R ²	q ₀ (mg.g ⁻¹)	R ²	E (kJ.mol ⁻¹)
0.31	.074	0.98	0.025	0.96	41.93	0.97	0.016

The Dubinin-Kaganer-Radushkevich isotherm (DKR) was also applied to the adsorption of Cd (II) metal ions onto NiO nanostructures. It assumes the adsorption process occurs both on homogeneous and heterogeneous surfaces. DR isotherm is presented in **Equation 7** [24, 32].

$$\ln q_e = \ln q_0 - k\varepsilon^2 \dots\dots\dots (7)$$

Where, q_e is the amount of metal ion adsorbed per unit weight of adsorbent (mmol.g⁻¹), q_0 is the DR monolayer adsorption capacity (mmol.g⁻¹), k is the activity coefficient related to adsorption energy (mol².kJ⁻²) and ε is the Polanyi potential which can be computed from **Equation 8** [32].

$$\varepsilon = RT \ln \left[1 + \frac{1}{C_e} \right] \dots\dots\dots (8)$$

The model parameters k and q_0 can be computed using the plots $\ln q_e$ versus ε^2 . Adsorption energy E (kJ.mol⁻¹) can be calculated using **Equation 9**[32].

$$E = \frac{1}{\sqrt{2k}} \dots\dots\dots (9)$$

The plot of $\ln q_0$ versus ε^2 for Cd (II) adsorption is shown in **Figure 3d**. The computed parameters of DR model are presented in **Table 3**. The E value for Cd (II) adsorption was found to be 1.13 kJ. mol⁻¹. The E value for metal ions adsorption is < 8 kJ.mol⁻¹ indicating the process is to be a physical-adsorption process [33].

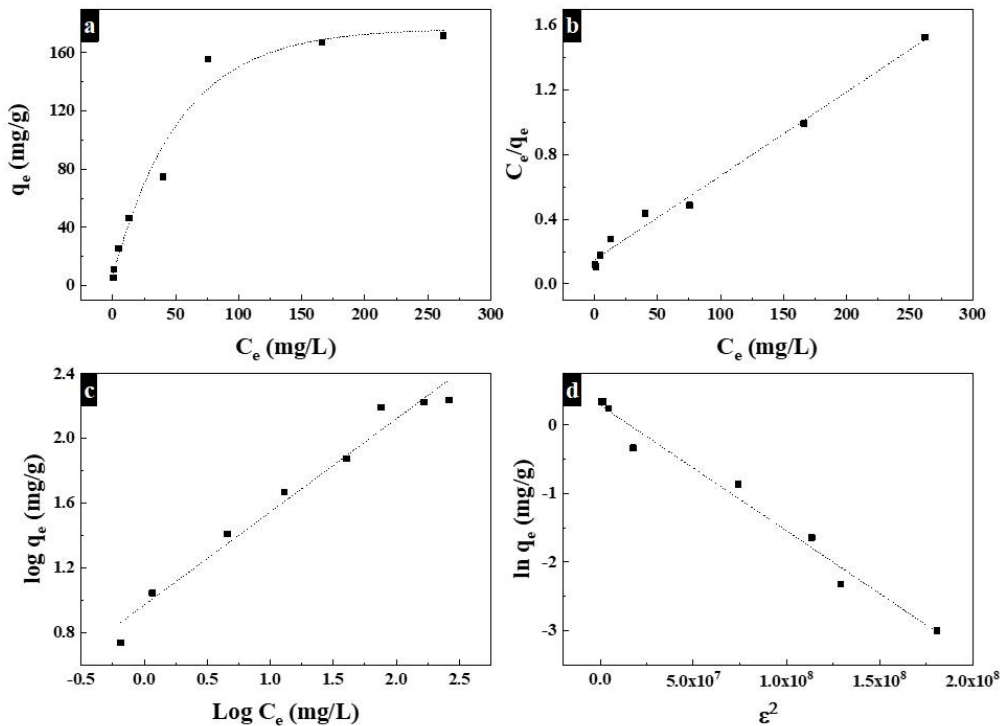


Figure 3:(a) Adsorption capacity of NiO at equilibrium versus initial concentration of Cd (II). (b) Langmuir isotherm, (c) Freundlich isotherm, and (d) DR model for the adsorption of Cd (II) on NiO.

CONCLUSION

A successful synthesis of NiO nanoparticle and their adsorption behavior towards heavy metal ions has been reported here. The nanomaterial was synthesized by the hydrothermal method followed by the calcination process. Structural characterizations of the hybrid were done using SEM, and spectroscopic characterizations were done using EDS and XRD spectrometer. Further, the nitrogen adsorption-desorption BET analysis indicated that the hybrid is mesoporous, having a surface area of $\sim 32.60 \text{ m}^2 \cdot \text{g}^{-1}$ and a pore diameter of $\sim 1.9 \text{ nm}$. The experimental results suggest that the adsorption process is physical and follows the Langmuir isotherm and pseudo-second-order model for metal ion adsorption in single and mixed solutions. Also, the adsorption process is spontaneous and primarily dominated by film diffusion. The NiO showed excellent adsorption of metal ions with a maximum adsorption capacity of $\sim 165 \text{ mg} \cdot \text{g}^{-1}$ for cadmium.

DECLARATIONS

The author declare no known competing financial interests or personal relationships that could have appeared to influence the work reported in this paper.

REFERENCES

1. S. Kumar, R.R. Nair, P.B. Pillai, S.N. Gupta, M.A.R. Iyengar, A.K. Sood, Graphene Oxide–MnFe₂O₄ Magnetic Nanohybrids for Efficient Removal of Lead and Arsenic from Water, *ACS Applied Materials & Interfaces* Vol. 6, pp. 17426-17436, 2014.
2. X. Zhao, B. Hu, J. Ye, Q. Jia, Preparation, Characterization, and Application of Graphene–Zinc Oxide Composites (G–ZnO) for the Adsorption of Cu(II), Pb(II), and Cr(III), *Journal of Chemical & Engineering Data* Vol. 58, pp. 2395-2401, 2013.
3. Y. Bian, Z.-Y. Bian, J.-X. Zhang, A.-Z. Ding, S.-L. Liu, H. Wang, Effect of the oxygen-containing functional group of graphene oxide on the aqueous cadmium ions removal, *Applied Surface Science* Vol. 329, pp. 269-275, 2015.
4. G. Zhao, X. Ren, X. Gao, X. Tan, J. Li, C. Chen, Y. Huang, X. Wang, Removal of Pb(II) ions from aqueous solutions on few-layered graphene oxide nanosheets, *Dalton Transactions* Vol. 40, pp. 10945-10952, 2011.
5. V. Mavrov, T. Erwe, C. Blöcher, H. Chmiel, Study of new integrated processes combining adsorption, membrane separation and flotation for heavy metal removal from wastewater, *Desalination* Vol. 157, pp. 97-104, 2003.
6. A. Dąbrowski, Z. Hubicki, P. Podkościelny, E. Robens, Selective removal of the heavy metal ions from waters and industrial wastewaters by ion-exchange method, *Chemosphere* Vol. 56, pp. 91-106, 2004.
7. [7] Q. Chen, Y. Yao, X. Li, J. Lu, J. Zhou, Z. Huang, Comparison of heavy metal removals from aqueous solutions by chemical precipitation and characteristics of precipitates, *Journal of Water Process Engineering* Vol. 26, pp. 289-300, 2018.
8. H.-C. Tao, T. Lei, G. Shi, X.-N. Sun, X.-Y. Wei, L.-J. Zhang, W.-M. Wu, Removal of heavy metals from fly ash leachate using combined bioelectrochemical systems and electrolysis, *Journal of Hazardous Materials* Vol. 264, pp. 1-7, 2014.
9. M.-q. Jiang, X.-y. Jin, X.-Q. Lu, Z.-l. Chen, Adsorption of Pb(II), Cd(II), Ni(II) and Cu(II) onto natural kaolinite clay, *Desalination* Vol. 252, pp. 33-39, 2010.
10. J. Zhu, S. Wei, H. Gu, S.B. Rapole, Q. Wang, Z. Luo, N. Haldolaarachchige, D.P. Young, Z. Guo, One-Pot Synthesis of Magnetic Graphene Nanocomposites Decorated with Core@Double-shell Nanoparticles for Fast Chromium Removal, *Environmental Science & Technology* Vol. 46, pp. 977-985, 2012.
11. M. Kobya, E. Demirbas, E. Senturk, M. Ince, Adsorption of heavy metal ions from aqueous solutions by activated carbon prepared from apricot stone, *Bioresource Technology* Vol. 96, pp. 1518-1521, 2005.
12. X. Luo, X. Lei, N. Cai, X. Xie, Y. Xue, F. Yu, Removal of Heavy Metal Ions from Water by Magnetic Cellulose-Based Beads with Embedded Chemically Modified Magnetite Nanoparticles and Activated Carbon, *ACS Sustainable Chemistry & Engineering* Vol. 4, pp. 3960-3969, 2016.
13. E. Erdem, N. Karapinar, R. Donat, The removal of heavy metal cations by natural zeolites, *Journal of Colloid and Interface Science* Vol. 280, pp. 309-314, 2004.
14. Ö. Yavuz, Y. Altunkaynak, F. Güzel, Removal of copper, nickel, cobalt and manganese from aqueous solution by kaolinite, *Water Research* Vol. 37, pp. 948-952, 2003.
15. A. Afkhami, M. Saber-Tehrani, H. Bagheri, Simultaneous removal of heavy-metal ions in wastewater samples using nano-alumina modified with 2,4-dinitrophenylhydrazine, *Journal of Hazardous Materials* Vol. 181, pp. 836-844, 2010.
16. I. Ali, New Generation Adsorbents for Water Treatment, *Chemical Reviews* Vol. 112, pp. 5073-5091, 2012.
17. Y. Yu, Y. Li, Y. Wang, B. Zou, Self-Template Etching Synthesis of Urchin-Like Fe₃O₄ Microspheres for Enhanced Heavy Metal Ions Removal, *Langmuir* Vol. 34, pp. 9359-9365, 2018.
18. E.-J. Kim, C.-S. Lee, Y.-Y. Chang, Y.-S. Chang, Hierarchically Structured Manganese Oxide-Coated Magnetic Nanocomposites for the Efficient Removal of Heavy Metal Ions from Aqueous Systems, *ACS Applied Materials & Interfaces* Vol. 5, pp. 9628-9634, 2013.
19. F. Rashidi, R.S. Sarabi, Z. Ghasemi, A. Seif, Kinetic, equilibrium and thermodynamic studies for the removal of lead (II) and copper (II) ions from aqueous solutions by nanocrystalline TiO₂, *Superlattices and Microstructures* Vol. 48, pp. 577-591, 2010.

20. L. Ai, Y. Zeng, Hierarchical porous NiO architectures as highly recyclable adsorbents for effective removal of organic dye from aqueous solution, *Chemical Engineering Journal* Vol. 215-216, pp. 269-278, 2013.
21. M. Qamar, M.A. Gondal, Z.H. Yamani, Synthesis of nanostructured NiO and its application in laser-induced photocatalytic reduction of Cr(VI) from water, *Journal of Molecular Catalysis A: Chemical* Vol. 341, pp. 83-88, 2011.
22. J. Zhao, Y. Tan, K. Su, J. Zhao, C. Yang, L. Sang, H. Lu, J. Chen, A facile homogeneous precipitation synthesis of NiO nanosheets and their applications in water treatment, *Applied Surface Science* Vol. 337, pp. 111-117, 2015.
23. Z.M. Khoshhesab, Z. Hooshyar, M. Sarfaraz, Removal of Pb(II) from Aqueous Solutions by NiO Nanoparticles, *Synthesis and Reactivity in Inorganic, Metal-Organic, and Nano-Metal Chemistry* Vol. 41, pp. 1046-1051, 2011.
24. Shivangi, S. Bhardwaj, T. Sarkar, Core-shell type magnetic Ni/NiO nanoparticles as recyclable adsorbent for Pb (II) and Cd (II) ions: One-pot synthesis, adsorption performance, and mechanism, *Journal of the Taiwan Institute of Chemical Engineers* Vol. 113, pp. 223-230, 2020.
25. N. Floquet, J.P. Coulomb, G. Weber, O. Bertrand, J.P. Bellat, Structural Signatures of Type IV Isotherm Steps: Sorption of Trichloroethene, Tetrachloroethene, and Benzene in Silicalite-I, *The Journal of Physical Chemistry B* Vol. 107, pp. 685-693, 2003.
26. L. Mouni, L. Belkhir, J.-C. Bollinger, A. Bouzaza, A. Assadi, A. Tirri, F. Dahmoune, K. Madani, H. Remini, Removal of Methylene Blue from aqueous solutions by adsorption on Kaolin: Kinetic and equilibrium studies, *Applied Clay Science* Vol. 153, pp. 38-45, 2018.
27. G.F. Malash, M.I. El-Khaiary, Piecewise linear regression: A statistical method for the analysis of experimental adsorption data by the intraparticle-diffusion models, *Chem. Eng. J.* Vol. 163, pp. 256-263, 2010.
28. M.A. Ahmad, R. Alrozi, Removal of malachite green dye from aqueous solution using rambutan peel-based activated carbon: Equilibrium, kinetic and thermodynamic studies, *Chemical Engineering Journal* Vol. 171, pp. 510-516, 2011.
29. J.U.K. Oubagaranadin, N. Sathyamurthy, Z.V.P. Murthy, Evaluation of Fuller's earth for the adsorption of mercury from aqueous solutions: A comparative study with activated carbon, *J. Hazard. Mater.* Vol. 142, pp. 165-174, 2007.
30. T. Sheela, Y.A. Nayaka, Kinetics and thermodynamics of cadmium and lead ions adsorption on NiO nanoparticles, *Chemical Engineering Journal* Vol. 191, pp. 123-131, 2012.
31. I.D. Mall, V.C. Srivastava, N.K. Agarwal, I.M. Mishra, Adsorptive removal of malachite green dye from aqueous solution by bagasse fly ash and activated carbon-kinetic study and equilibrium isotherm analyses, *Colloids and Surfaces A: Physicochemical and Engineering Aspects* Vol. 264, pp. 17-28, 2005.
32. J.P. Hobson, Physical adsorption isotherms extending from ultrahigh vacuum to vapor pressure, *The Journal of Physical Chemistry* Vol. 73, pp. 2720-2727, 1969.
33. W. Ma, F.-Q. Ya, M. Han, R. Wang, Characteristics of equilibrium, kinetics studies for adsorption of fluoride on magnetic-chitosan particle, *J. Hazard. Mater.* Vol. 143, pp. 296-302, 2007.

CITATION OF THIS ARTICLE

Pratima Rani Sardar. Green synthesis of nickel oxide nanoparticles and its adsorption isotherm and kinetics studies for heavy metal ions removal. *Bull. Env.Pharmacol. Life Sci.*, Vol10[9] August 2021 :08-15